



# Characteristic Evaluation of Pressure Mapping System for Patient Position Monitoring in Radiation Therapy

Seonghee Kang<sup>1,2,3</sup>, Chang Heon Choi<sup>1,2,3</sup>, Jong Min Park<sup>1,2,3</sup>, Jin-Beom Chung<sup>4</sup>, Keun-Yong Eom<sup>4</sup>,  
Jung-in Kim<sup>1,2,3</sup>

<sup>1</sup>Department of Radiation Oncology, Seoul National University Hospital, <sup>2</sup>Institute of Radiation Medicine, Seoul National University Medical Research Center, <sup>3</sup>Biomedical Research Institute, Seoul National University Hospital, Seoul, <sup>4</sup>Department of Radiation Oncology, Seoul National University Bundang Hospital, Seongnam, Korea

**Received** 1 December 2021  
**Revised** 13 December 2021  
**Accepted** 15 December 2021

**Corresponding author**  
Jung-in Kim  
(madangin@gmail.com)  
Tel: 82-2-2072-3573  
Fax: 82-2-765-3317

**Purpose:** This study evaluated the features of a pressure mapping system for patient motion monitoring in radiation therapy.

**Methods:** The pressure mapping system includes an MS 9802 force sensing resistor (FSR) sensor with 2,304 force sensing nodes using 48 columns and 48 rows, controller, and control PC (personal computer). Radiation beam attenuation caused by pressure mapping sensor and signal perturbation by 6 and 10 mega voltage (MV) photon beam was evaluated. The maximum relative pressure value (mRPV), average relative pressure value (aRPV), the center of pressure (COP), and area of pressure distribution were obtained with/without radiation using the upper body of an anthropomorphic phantom for 30 minutes with 15 MV.

**Results:** It was confirmed that the differences in attenuation induced by the FSR sensor for 6 and 10 MV photon beams were small. The differences in mRPV, aRPV, area of pressure distribution with/without radiation are about 0.6%, 1.2%, and 0.5%, respectively. The COP values with/without radiation were also similar.

**Conclusions:** The characteristics of a pressure mapping system during radiation treatment were evaluated on the basis of attenuation and signal perturbation using radiation. The pressure distribution measured using the FSR sensor with little attenuation and signal perturbation by the MV photon beam would be helpful for patient motion monitoring.

**Keywords:** Pressure mapping system, Pressure distribution, Motion management, Patient setup, Real-time motion monitoring

## Introduction

Accurate delivery of radiotherapy is affected by different geometrical uncertainties, such as inter-fraction variation, intra-fractional motion, changes to the target volume, and patient setup errors [1-3]. To improve the treatment outcome, particularly when combined with highly conformal delivery techniques, such as intensity-modulated radiation therapy and volumetric-modulated arc therapy, which are

often accompanied by steep dose gradient, different technologies have been developed to obtain the patient's image daily and/or during treatment. [4-6].

Various image guidance technologies to improve patient positioning have been suggested by researchers, including kilo-voltage (kV) X-ray imaging, in-room computed tomography (CT), kV, and mega voltage (MV) cone-beam CT (CBCT) [7-9]. These techniques enables the ability to visualize the patient anatomy directly with submillimeter

accuracy and match the patient's initial planned position. However, imaging methods based on ionizing radiation deliver additional doses to the patient, and the imaging dose is not currently accounted for in treatment planning [9]. Other image guidance techniques, including infrared, optical, and radiofrequency based technologies that do not use ionizing radiation have also been proposed to monitor patient setup and intra-motion [10-12]. These techniques provide patient setup position, real-time motion monitoring, and surrogate respiratory signal without additional imaging dose [11,13]. However, patient surface or marker should be visible to monitor the patient's position, and gantry, imaging arms can block the camera's view.

The pressure mapping technique is widely used in different fields such as health care, industrial, and robotics [14]. It provides quantitative information on human posture and movement, such as balance and foot-ground interaction, which is a fundamental aspect for evaluating the quality of life in health care [15]. Among the different pressure sensors, force sensing resistor (FSR) sensor comprised of conductive particles in the polymer matrix has better impact resistance and durability. Also, it can be produced in different ranges of size, shape, and arrangement. The FSR sensor has a very thin and light film structure with excellent repeatability and accuracy [14,15]. Shieh et al. [16] developed an oropharyngeal swallowing monitoring system that can be wearable and portable using an FSR sensor. Cho et al. [17] reported the immobilization-device quality assurance system, which could measure the force between a patient and the thermoplastic mask quantitatively using an FSR sensor. Additionally, a patient alignment method that measures the pressure distribution between patient's back and treatment table was proposed to enhance patient setup accuracy [18]. However, the characteristic evaluation of signal perturbation, incident beam attenuation, and position accuracy tests of the measured pressure distribution during the MV photon beam delivery has not yet been performed. Therefore, performs the characteristic evaluation of pressure mapping systems for patient position verification in radiation therapy.

## Materials and Methods

### 1. System configuration

The pressure mapping system includes MS 9802 FSR sensor (Kitronyx Inc, Seoul, Korea), which has 2,304 force sensing nodes using 48 columns and 48 rows, Baikal force controller (Kitronyx Inc), and control PC (personal computer), as indicated in Fig. 1. The sensing area of the FSR sensor is 454×693 mm<sup>2</sup>, and thickness is 0.62 mm. The change in internal resistance corresponding to the applied mechanical stress is converted into electrical signal using the FSR sensor. The electrical signal is transformed into the digital signal by a controller with a USB interface acting as a series port, enabling it to be controlled by the control PC. It can measure the maximum pressure up to 4 kg/cm<sup>2</sup>, and the available temperature range is -20 to 60 degrees. The sampling rate of the pressure mapping system was up to 32 Hz. The transmitted signal can be displayed in real-time using the software and quantitative analysis, such as three-dimensional (3D) pressure distribution, the center of pressure (COP), maximum relative pressure value (mRPV), average relative pressure value (aRPV), and the area is possible. COP location is identified from the voltage signals received from the sensing nodes. The pressure distribution varies along the sensing nodes and time. With the finite sensing nodes lateral direction limits (a, b) and longitudinal direction limits (c, d), the real-time centroid of the distributed dynamic pressure,  $p(x, y, t)$ , along the lateral (x) or longitudinal (y) directions is given as the following equation (1) and (2):

$$COP_{lat}(t) = \frac{\int_c^d \int_a^b x \cdot p(x,y,t) dx dy}{\int_c^d \int_a^b p(x,y,t) dx dy} \quad (1)$$

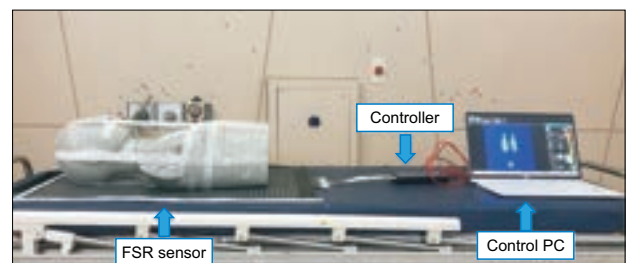


**Fig. 1.** System configuration of the pressure mapping system. FSR, force sensing resistor; PC, personal computer.

$$\text{COP}_{\text{Ing}}(t) = \frac{\int_c^d \int_a^b y \cdot p(x,y,t) \, dx dy}{\int_c^d \int_a^b p(x,y,t) \, dx dy} \quad (2)$$

These definitions of the  $\text{COP}_{\text{lat}}(t)$  and  $\text{COP}_{\text{Ing}}(t)$  provide the total pressure at time  $t$  and the ratio relative to the pressure center location along with a continuously distributed sensor [19].

## 2. Characteristic evaluation in the radiation field

Both the radiation beam attenuation caused by pressure mapping sensor and signal perturbation by MV photon beam was evaluated. 6 MV and 10 MV photon beams were delivered using VitalBEAM (Varian Medical Systems, Palo Alto, CA, USA) at the reference setup with the source to surface distance (SSD; 100 cm, field size  $10 \times 10 \text{ cm}^2$ ) with gantry  $0^\circ$ . Attenuation was defined as the ratio of the radiation dose with/without the device. Integrated coulomb measurement at a depth of the maximum dose ( $D_{\text{max}}$ ) was performed using a Farmer type chamber (TN 30013; PTW, Freiburg, Germany) and an electrometer (Unidose E, PTW) in a solid water phantom. 100 MU (monitor unit) and 500 MU were delivered twice to reduce inter-measurement variation. Signal perturbation was evaluated using extended SSD 400 cm, 15 MV photon beam with  $40 \times 40 \text{ cm}^2$  and 3,000 MU. The measurement in the extended SSD was performed to consider the total body irradiation (TBI), which delivers

the beam with a low dose rate ( $<10 \text{ cGy/min}$ ). The mRPV, aRPV, COP, and area were obtained with/without radiation using the upper body of an anthropomorphic phantom (Model 702 Adult ATOM Female; CIRS Inc., Norfolk, VA, USA) for 30 minutes, as indicated in Fig. 2. Additionally, COP was measured at 10 minutes intervals to confirm the position change due to signal fluctuation by radiation.

## 3. Comparison for positioning accuracy using cone-beam computed tomography

To evaluate the accuracy of the COP measured using a pressure mapping sensor, it was compared with CBCT, which is integrated into a linear accelerator and capable of acquiring 3D volumetric image. The multi-imaging modality iso-centricity (MIMI) phantom (Standard Imaging, Middleton, WI, USA) obtained by the Brilliance CT Big Bore<sup>TM</sup> (Philips, Amsterdam, Netherlands) was used as a reference image to match the CBCT image. The MIMI phantom was placed on the treatment couch, and aligning the phantom was performed at a known offset (lateral: 1.2 cm, longitudinal: 1.0 cm) position using the external lasers. Here, the COP value was obtained by placing the pressure mapping sensor between the treatment couch and the MIMI phantom. After obtaining the CBCT image of the MIMI phantom with the known offset, the offset vectors were calculated through registration with the reference image. To compare

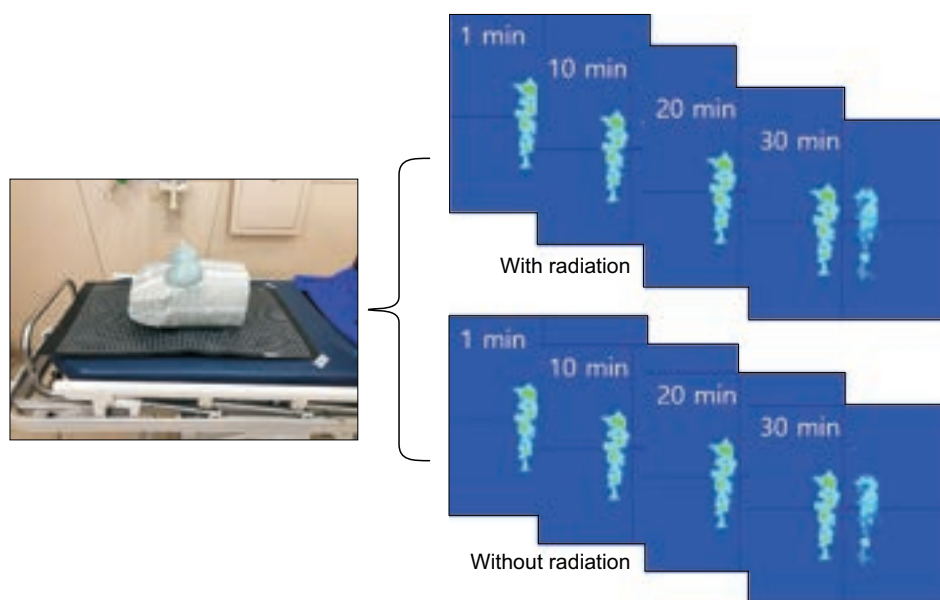


**Fig. 2.** Pressure distribution acquisition during 30 minutes without radiation and with 15 MV photon beam, dose rate 100 MU/min. MU, monitor unit.

the vector values and COP value obtained using the offset, the image without the offset was obtained to calculate the vectors and COP values.

## Results and Discussion

The characteristics of the pressure mapping system were evaluated in the situation where MV photon beam is delivered to confirm whether it is possible or not to apply patient motion management during treatment. Before applying clinical implementation, it should be confirmed that there is no effect such as signal fluctuation and attenuation by the incident beam.

There are different types of pressure mapping sensors, such as piezo-resistive, capacitance, and piezoelectricity, and the FSR sensor used in this study piezo-resistive study, can be used with relatively simpler electronics at high-speed, is very thin. The attenuation of the incident beam differs depending on the thickness and components of the sensor, and the signal measured using the sensor could be altered by radiation. If the sensor is affected by radiation, the sensor is unsuitable for patient motion monitoring for radiation therapy. Therefore, to monitor the patient's motion during treatment, the characteristic evaluation for the MV photon beam should be conducted.

As indicated in Table 1, the difference in the measured charge with and without the FSR sensor at 6 MV was 0.1% and 0.06% at 100 MU and 500 MU, respectively, and it was 0.05% at 100 MU and 0.1% at 500 MU in 10 MV photon beam. It was confirmed that the difference in attenuation caused by the FSR sensor for both energies was small. Sep-

pälä and Kulmala [20] reported that the attenuation caused by the carbon fiber couch was about 3.6% at 6 MV and about 2.4% at 15 MV; it should be appropriately reflected in the treatment plan due to the increase in skin dose. However, in the case of the sensor used in this study, the increase in skin dose is expected to be insignificant because there is little attenuation effect.

Table 2 indicates the mRPV, aRPV, and area of pressure distribution with and without radiation for 30 minutes in a 15 MV beam. The difference in mRPV, aRPV, area of pressure distribution with/without radiation is about 0.6%, 1.2%, and 0.5%, respectively. The COP values were also confirmed that there was little difference between when the radiation was delivered or not, as indicated in Table 3. There is little radiation effect on the pressure distribution of the anthropomorphic phantom measured at 10 minutes intervals. In the case of external beam radiation therapy, including stereotactic body radiation therapy, the beam delivery time is less than ten minutes, but if treatment was conducted, such as TBI with a low dose rate for a long time, it takes more than 30 minutes. Therefore, the effect of radiation during 30 minutes in TBI condition needs to be confirmed, and the results show that there is no significant difference.

**Table 2.** mRPV, aRPV, and area of pressure distribution without and with radiation for 30 minutes in 15 MV beam

|                         | With radiation | Without radiation | Difference (%) |
|-------------------------|----------------|-------------------|----------------|
| mRPV                    | 167            | 166               | 0.6            |
| aRPV                    | 46.43          | 45.86             | 1.2            |
| Area (cm <sup>2</sup> ) | 242.99         | 241.67            | 0.5            |

mRPV, maximum relative pressure value; aRPV, average relative pressure value.

**Table 1.** Evaluation of attenuation by FSR sensor with 100 MU and 500 MU, field size 10×10 cm<sup>2</sup>

|                | 100 MU       |              |              | 500 MU       |              |              |
|----------------|--------------|--------------|--------------|--------------|--------------|--------------|
|                | 1st rdg (nC) | 2nd rdg (nC) | Average (nC) | 1st rdg (nC) | 2nd rdg (nC) | Average (nC) |
| 6 MV           |              |              |              |              |              |              |
| Without        | 3.294        | 3.295        | 3.295        | 16.48        | 16.49        | 16.49        |
| With           | 3.298        | 3.298        | 3.298        | 16.49        | 16.50        | 16.50        |
| Difference (%) |              |              | 0.1          |              |              | 0.06         |
| 10 MV          |              |              |              |              |              |              |
| Without        | 3.368        | 3.366        | 3.367        | 16.83        | 16.83        | 16.83        |
| With           | 3.368        | 3.369        | 3.369        | 16.85        | 16.85        | 16.85        |
| Difference (%) |              |              | 0.05         |              |              | 0.1          |

FSR, force sensing resistor; MU, monitor unit; rdg, reading.

**Table 3.** Center of pressure variation for 30 minutes without and with radiation

| Time (min) | With radiation |           | Without radiation |           |
|------------|----------------|-----------|-------------------|-----------|
|            | Lat. (cm)      | Lng. (cm) | Lat. (cm)         | Lng. (cm) |
| 1          | -1.21          | 1.10      | -1.23             | 1.11      |
| 10         | -1.22          | 1.12      | -1.23             | 1.17      |
| 20         | -1.22          | 1.13      | -1.23             | 1.10      |
| 30         | -1.23          | 1.07      | -1.21             | 1.09      |

Lat., lateral; Lng., longitudinal.

Table 4 indicates the results of the positioning accuracy compared with CBCT. There is a difference between 1.2 mm and 1.1 mm for lateral and longitudinal directions between CBCT and pressure mapping system, respectively. The node spacing of the FSR sensor is 0.95 mm and 1.45 mm for lateral and longitudinal direction, making it challenging to ensure the accuracy of the sub millimeters exhibited in X-ray or surface-based monitoring systems. However, the pressure distribution can acquire real-time information caused by a patient's lying position, which cannot be obtained from a surface-guided or X-ray based monitoring system. Although it was confirmed that the self-correction method using patient's backpressure distribution helps improve the patient's setup, different effects using MV photon beam were not evaluated [18].

Patient motion monitoring using pressure distribution is a novel application that has not been widely used in radiation therapy and can acquire information such as lying position, patient's weight, which cannot be verified in existing devices. However, these systems should be evaluated for features in the environment where treatment is performed before clinical use, and it was confirmed that the signal perturbation by radiation and attenuation measured using the pressure mapping system was small. Our results confirmed the possibility of acquiring the pressure distribution during radiation therapy, and in the future, motion monitoring will be conducted through volunteer and patient case studies to evaluate the possibility of clinical implementation.

## Conclusions

In this study, the characteristics of a pressure mapping technique during treatment were evaluated in terms of attenuation and signal perturbation using radiation. The

**Table 4.** Positioning verification using CBCT and MIMI phantom

|            | Lat. (cm) | Lng. (cm) |
|------------|-----------|-----------|
| CBCT       | 1.16      | 1.00      |
| FSR sensor | 1.04      | 1.11      |
| Difference | 0.12      | 0.11      |

CBCT, cone-beam computed tomography; MIMI, multi-imaging modality iso-centricity; FSR, force sensing resistor; Lat., lateral; Lng., longitudinal.

pressure distribution measured using the FSR sensor with a thickness of 0.6 mm was confirmed to have little attenuation and signal perturbation by the MV photon beam. The pressure distribution would be suitable for patient motion management methods during radiation therapy because it can monitor real-time movement and information for the lying position, which is hard to obtain in the existing system. Based on these results, clinical implementation by applying pressure the mapping technique to volunteers and patients will be further conducted.

## Acknowledgements

This work was supported by the National Research Foundation of Korea (NRF) grant funded by the Korea Government (Ministry of Science and ICT, MSIT) (No. 2020R1C1C100936611) and by SNUH Research Fund (No. 0420210620).

## Conflicts of Interest

The authors have nothing to disclose.

## Availability of Data and Materials

All relevant data are within the paper and its Supporting Information files.

## Author Contributions

Conceptualization: Seonghee Kang and Keun-Yong Eom. Data curation: Seonghee Kang. Formal analysis: Chang Heon Choi and Jong Min Park. Methodology: Jin-Beom Chung. Project administration: Jung-in Kim. Writing—original draft: Seonghee Kang. Writing—review & editing: Jung-in Kim.

## References

1. Keall PJ, Mageras GS, Balter JM, Emery RS, Forster KM, Jiang SB, et al. The management of respiratory motion in radiation oncology report of AAPM Task Group 76. *Med Phys.* 2006;33:3874-3900.
2. Kang SH, Yoon JW, Kim TH, Suh TS. Development of respiratory training system using individual characteristic guiding waveform. *Korean J Med Phys.* 2012;23:1-7.
3. Shin DS, Kang SH, Kim DS, Kim TH, Kim KH, Cho MS, et al. Evaluating correlation between geometrical relationship and dose difference caused by respiratory motion using statistical analysis. *Prog Med Phys.* 2016;27:203-212.
4. Kim JI, Choi CH, Park SY, An H, Wu HG, Park JM. Gamma evaluation with portal dosimetry for volumetric modulated arc therapy and intensity-modulated radiation therapy. *Prog Med Phys.* 2017;28:61-66.
5. Zhang P, Happersett L, Hunt M, Jackson A, Zelefsky M, Mageras G. Volumetric modulated arc therapy: planning and evaluation for prostate cancer cases. *Int J Radiat Oncol Biol Phys.* 2010;76:1456-1462.
6. Studenski MT, Bar-Ad V, Siglin J, Cognetti D, Curry J, Tuluc M, et al. Clinical experience transitioning from IMRT to VMAT for head and neck cancer. *Med Dosim.* 2013;38:171-175.
7. Siewerdsen JH, Jaffray DA. Cone-beam computed tomography with a flat-panel imager: magnitude and effects of x-ray scatter. *Med Phys.* 2001;28:220-231.
8. Siewerdsen JH, Moseley DJ, Burch S, Bisland SK, Bogaards A, Wilson BC, et al. Volume CT with a flat-panel detector on a mobile, isocentric C-arm: pre-clinical investigation in guidance of minimally invasive surgery. *Med Phys.* 2005;32:241-254.
9. Murphy MJ, Balter J, Balter S, BenComo JA Jr, Das IJ, Jiang SB, et al. The management of imaging dose during image-guided radiotherapy: report of the AAPM Task Group 75. *Med Phys.* 2007;34:4041-4063.
10. Freislederer P, Kügele M, Öllers M, Swinnen A, Sauer TO, Bert C, et al. Recent advanced in Surface Guided Radiation Therapy. *Radiat Oncol.* 2020;15:187.
11. Placht S, Stancanello J, Schaller C, Balda M, Angelopoulou E. Fast time-of-flight camera based surface registration for radiotherapy patient positioning. *Med Phys.* 2012;39:4-17.
12. Zhao B, Maquilan G, Jiang S, Schwartz DL. Minimal mask immobilization with optical surface guidance for head and neck radiotherapy. *J Appl Clin Med Phys.* 2018;19:17-24.
13. Xiao A, Crosby J, Malin M, Kang H, Washington M, Hasan Y, et al. Single-institution report of setup margins of voluntary deep-inspiration breath-hold (DIBH) whole breast radiotherapy implemented with real-time surface imaging. *J Appl Clin Med Phys.* 2018;19:205-213.
14. Al-Handarish Y, Omisore OM, Igbe T, Han S, Li H, Du W, et al. A survey of tactile-sensing systems and their applications in biomedical engineering. *Adv Mater Sci Eng.* 2020;2020:4047937.
15. Saenz-Cogollo JF, Pau M, Fraboni B, Bonfiglio A. Pressure mapping mat for tele-home care applications. *Sensors (Basel).* 2016;16:365.
16. Shieh WY, Wang CM, Chang CS. Development of a portable non-invasive swallowing and respiration assessment device. *Sensors (Basel).* 2015;15:12428-12453.
17. Cho MS, Kim TH, Kang SH, Kim DS, Kim KH, Shin DS, et al. A noble technique a using force-sensing resistor for immobilization-device quality assurance: a feasibility study. *J Korean Phys Soc.* 2016;68:803-809.
18. Kim TH, Kang SH, Kim DS, Cho MS, Kim KH, Suh TS, et al. Feasibility study of patient motion monitoring by using tactile array sensors. *J Korean Phys Soc.* 2015;67:199-203.
19. Yoo B, Pines DJ. Development of two-dimensional interdigitated center of pressure sensor. *Smart Mater Struct.* 2017;26:125013-125027.
20. Seppälä JK, Kulmala JA. Increased beam attenuation and surface dose by different couch inserts of treatment tables used in megavoltage radiotherapy. *J Appl Clin Med Phys.* 2011;12:3554.